

Growth of CuFeO₂ Single Crystals by the Optical Floating-Zone Technique

Nora Wolff^{a,b,*}, Tobias Schwaigert^a, Dietmar Siche^a, Darrell G. Schlom^{c,d}, and Detlef Klimm^a

^aLeibniz-Institut für Kristallzüchtung, Max-Born-Str. 2, 12489 Berlin, Germany

^bHelmholtz-Zentrum Berlin für Materialien und Energie, Hahn-Meitner-Platz 1, 14109 Berlin, Germany

^cDepartment of Materials Science and Engineering, Cornell University, Ithaca, NY 14853-1501, USA

^dKavli Institute at Cornell for Nanoscale Science, Ithaca, NY 14853-1501, USA

Abstract

CuFeO₂ single crystals up to 50 mm in length and up to 10 mm in diameter were grown by the optical floating-zone method. Stoichiometric polycrystalline rods with a diameter of 6–12 mm were used as feed materials to produce crystals of sufficient size to be used as substrates for the growth of thin films of delafossites. For stable growth along the *c*-axis, low growth rates of 0.4 mm/h are necessary. Due to the incongruent melting behavior of CuFeO₂, a stable melt zone requires adjustment of the lamp power during growth. The melting of CuFeO₂ is not simply incongruent because the thermodynamic equilibrium includes more than two solid phases and the melt; the gas phase is also involved. The crystals were characterized by X-ray diffraction and X-ray fluorescence measurements.

Keywords: A1. Phase equilibria, A1. Substrates, A2. Floating zone technique, B1. Oxides

1. Introduction

While examining the mineralogical collection of the École Nationale des Mines in Paris, Charles Friedel found an artifact claimed to be “Graphite

*Corresponding author

Email address: nora.wolff@helmholtz-berlin.de (Nora Wolff)

from Catherineburgh, Sibiria” — which instead he reported in the year 1873 to be composed from equimolar quantities of Cu_2^+O with the combination of $\text{Fe}_2^{3+}\text{O}_3$, about 3.5% Al_2O_3 [1]. This chemical composition can be written as $\text{Cu}(\text{Fe,Al})\text{O}_2$. The new mineral was given the name delafossite. In the years since Friedel’s discovery a large number of other $\text{A}^+\text{B}^{3+}\text{O}_2$ compounds have become known that show basically the same structural features: BO_6 octahedra form layers that are stacked parallel to (001), and these edge-sharing octahedral sheets are connected along the [001] direction by linear $\text{O}-\text{A}^+-\text{O}$ bonds. Depending on details of the stacking sequence, the structures are usually either hexagonal or trigonal [2]. As an exception, $\text{Cu}^+\text{Mn}^{3+}\text{O}_2$ is monoclinic with space group $C2/m$ [3]. Shannon et al. [4] revealed that not only copper and silver can act as the A^+ element, but also other quite noble metals like palladium or even platinum. This is surprising because oxides of the platinum group metals are not only scarce and often unstable, but also the known platinum group binary oxides show oxidation states of 2+ or higher, e.g. PdO , PdO_2 , PtO , PtO_2 , PtO_3 , and not Pt^{1+} as occurs in Pt-containing delafossites.

Oxide materials based on the ABO_2 delafossite structure are of particular interest due to the novel properties that accompany their cation variation at A and B sites. These properties are of interest to fundamental science [5, 6, 7, 8, 9] as well as applications [10]. Usually, the semiconductor delafossites consist of Ag or Cu at the A-site and several trivalent cations like Al, Fe or Ga at the B-site. Important among the semiconducting delafossites is CuAlO_2 with its relatively high mobility for a p-type transparent conducting oxide [11]. Pd- and Pt-based compounds (for A^+) are metallic delafossite oxides where B-site cations are transition metals like Co, Cr or Rh [4, 12, 13]. Among these, the growth of single crystalline PdCoO_2 has become of interest due to its ultra-high conductivity at room temperature. Recently an in-plane resistivity $\rho_{ab} = 2.6 \mu\Omega\cdot\text{cm}$ at 295 K was measured for sub-mm-sized PdCoO_2 crystals, which makes this material the most conductive oxide known, comparable to the best metallic conductors Ag, Cu, Au and Al [5]. Even though it is a platinum group oxide, this material has a fairly high thermal stability up to 900 °C [4].

The excellent properties exhibited by delafossites, including a mean-free path of about $20\mu\text{m}$ at low temperature in PdCoO_2 , [5] invites the growth of delafossite heterostructures. In such heterostructures bandgap engineering [14], strain engineering [15], symmetry breaking and other thin-film approaches could be applied to modify the properties of delafossites as has become commonplace for other oxides [16]. Unfortunately, there are no commercially available delafossite substrates.

So far, epitaxial layers have mainly been grown on sapphire substrates [17, 18, 19] – unfortunately with significantly degraded quality resulting from the not well matched crystallographic lattice of sapphire ($R\bar{3}c$, $a = 4.7602\text{ \AA}$, $c = 12.9933\text{ \AA}$ [20]) and PdCoO_2 ($R\bar{3}m$ $a = 2.830\text{ \AA}$, $c = 17.743\text{ \AA}$ [6]). The resulting delafossite films contain in-plane rotation twins and other defects that result in the best of today’s PdCoO_2 films [17] having resistivities at room temperature 1.8 times higher than PdCoO_2 single crystals [21] and 145 times higher resistivities at 4 K. For the growth of high quality epitaxial layers, isostructural single crystalline substrates with similar lattice constants are required.

The aim of this work is to grow relatively large delafossite crystals that in subsequent studies can be used as substrates for the growth of high quality delafossite films. According to the structural parameters, CuAlO_2 ($R\bar{3}m$, $a = 2.8571\text{ \AA}$, $c = 16.940\text{ \AA}$ [4]) would be the most suitable substrate material for PdCoO_2 . Unfortunately, the melt growth of bulk CuAlO_2 crystals with sufficient size is impossible, because the substance melts peritectically under the formation of solid Al_2O_3 and the growth window (= CuAlO_2 liquidus) between the peritectic and eutectic points is too small [22, 23]. The melting points of iron oxides (Fe_2O_3 decomposes to Fe_3O_4 , which melts at 1597°C) are significantly lower than for Al_2O_3 ($T_f = 2054^\circ\text{C}$ [24]), and consequently a larger growth window for CuFeO_2 ($R\bar{3}m$, $a = 3.0351\text{ \AA}$, $c = 17.166\text{ \AA}$) can be expected. (Some $\text{CuO-Fe}_2\text{O}_3$ phase diagrams [25, 26] in the literature neglect the decomposition of Fe_2O_3 and show the congruent melting point of Fe_3O_4 instead.) CuFeO_2 is the only delafossite compound, that has already be grown with reasonable quality in diameters up to 5–8 mm by the optical floating zone (OFZ) technique

[25, 27, 28].

So far CuFeO_2 single crystals have been grown from stoichiometric sintered rods by the OFZ technique. Our prior thermodynamic investigations have shown that growth methods involving crucibles are unsuitable as the aggressive copper melt attacks all crucible materials [22]. In addition to pure CuFeO_2 , $\text{CuFe}_{1-x}\text{Ga}_x\text{O}_2$ with $x \leq 12\%$ have been grown by Song et al. by the OFZ method [26]. For $\text{CuCr}_{1-x}\text{Al}_x\text{O}_2$ it was shown that solid solution formation with mixed occupancy on the B-site seems to stabilize the delafossite phase thermodynamically [29], but CuFeO_2 with high ($\approx 30\%$) Al^{3+} content only grew in polycrystalline form, presumably as a result of severe segregation in the CuFeO_2 – CuAlO_2 solid solution system. The present work focuses on the growth of pure CuFeO_2 with sufficient size and perfection to be useful for delafossite substrates. We show that the oxygen fugacity p_{O_2} in the gas phase acts on the equilibria between the relevant oxidation states of copper (+2, +1, 0) and iron (+3, +2) — which then influences the crystallization behavior of delafossites.

2. Experimental

Growth experiments were carried out in an OFZ furnace from Crystal System Corporation (type FZ-T-10000-H-VII-VPO-PC). The equipment has a four-mirror setup with 1000 W or 1500 W halogen lamps and a fused silica protection tube. An argon flow of 0.31 min^{-1} with 5N purity and total pressure of 1 atm was used as the growth atmosphere, to stabilize the CuFeO_2 phase [23]. The seed and feed rods were rotated at 15 rpm in opposite directions, and pulling rates between 0.4 and 1.1 mm h^{-1} were employed. Due to the incongruent melting, the lamp power was decreased slowly during the first 5-10 h of the experiments.

To prepare the rods, vacuum-dried powders of Cu_2O (Fox Chemicals, 4N purity) and Fe_2O_3 (Alfa Aesar, 4N8 purity) in 1:1 molar ratio were mixed and sintered for 25 h at 900°C in 1 atm of argon. XRD powder analysis confirmed that a pure delafossite phase resulted from this annealing process. Following grinding of the sintered CuFeO_2 , the powder was compacted in a plastic bag and

pressed for 3 min at 2 kbar at room temperature in a cold isostatic press from Engineered Pressure International NV, Belgium. To increase the density, the pressed block was again sintered for 8 h at 900 °C in argon. Rods with diameters of 6, 8 and 12 mm and 120 mm length were drilled out of the sintered blocks with a core drill. The density of the rods was 70-80% of the theoretical value. The grown crystals were characterized by X-ray diffraction (XRD), energy-dispersive Laue mappings (EDLM) and X-ray fluorescence (XRF) spectroscopy. The latter were performed using a μ -XRF spectrometer M4 Tornado (Bruker). Laue method was used to orient the crystals and prepare planar substrates oriented perpendicular to the *c*-axis.

3. Results

Five growth experiments were performed that are summarized in Table 1. In order to optimize the quality and size of the crystals, the diameter of the polycrystalline source rods was increased and the growth rate was reduced in the later growth experiments. Due to the incongruent melting of the compound, slow growth rates $< 0.4 \text{ mm h}^{-1}$ are preferable and gave the best results. In addition, lower growth rates facilitate the transport of oxygen gas from the environment to the growth interface to oxidize the iron ($\text{Fe}^{2+} \rightarrow \text{Fe}^{3+}$), as is discussed in the next section. Higher growth rates lead to polycrystalline growth, and the crystal orientation during the growth experiment often changes. At low growth rate the *c* axis is the prevailing growth direction. Occasional changes in growth orientation are clearly visible on the crystal surface of the grown rod because the (001) planes of the delafossite are shiny and the others appear dull. This means that a crystal that is grown along [001] should not have a shiny lateral surface. In contrast to recent observations during the growth of CuLaO_2 delafossite in pure argon [30], no outer ring containing Cu^{2+} was observed in our experiments with CuFeO_2 .

Fig. 1 shows a rod that was grown with a high growth rate of 1.1 mm h^{-1} . In order to visualize the single crystalline regions and composition, the rod

was sawn along its axis and investigated by EDLM. Elemental maps of the cross sections revealed a composition close to the stoichiometric of the grown material. Spatial mapping of a Bragg peak (EDLM), showed that only the tail end of the grown rod is a single crystal [31].

Table 1: OFZ growths experiments with CuFeO_2 . d – rod diameter, v – growth rate, P – lamp power.

Grown Rod #	d (mm)	v (mm h^{-1})	P (W)	remarks
1	6	1.1	1000	Fig. 1
2	8	0.55	1000	Fig. 2a)
3	8	0.4	1000	Fig. 2b)
4 & 5	12	0.4	1500	Fig. 3, best results

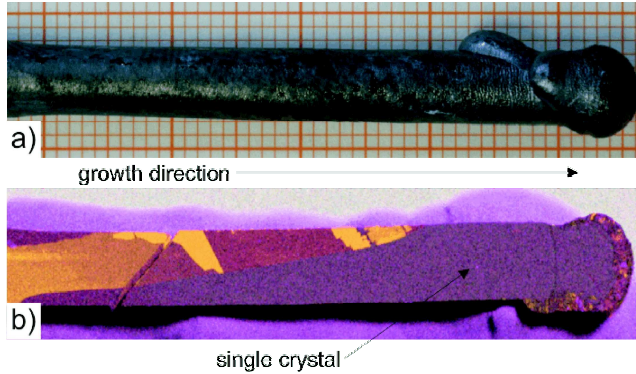


Figure 1: a) CuFeO_2 grown rod #1 (cf. Table 1). b) EDLM results of the same rod sectioned parallel to the growth direction.

The reduction of the growth rate to 0.55 mm h^{-1} and then to 0.4 mm h^{-1} resulted in significantly better crystal quality (Fig. 2a) and b), respectively). With a growth rate of 0.4 mm h^{-1} , the change in crystal orientation during the growth process could be avoided. Even though the c -axis is slightly tilted with respect to the growth direction (part of the lateral surface is shiny), the longest delafossite single crystal known to date was grown.

The handling of larger diameters $\geq 10 \text{ mm}$ is more difficult because the sur-

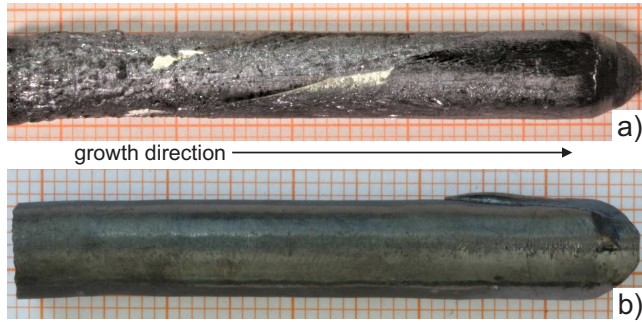


Figure 2: a) CuFeO_2 rod #2. b) CuFeO_2 rod #3 (cf. Table 1).

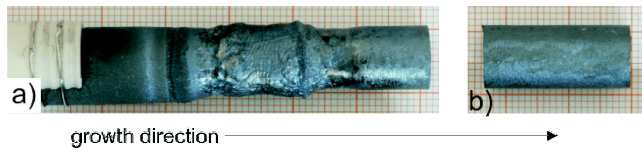


Figure 3: a) Unstable growth of CuFeO_2 in the initial growth state of rod #5 (cf. Table 1). b) Single crystal part of the same rod.

face tension of the larger melt zone is less stable, resulting in overflow (Fig. 3a)). Stable growth became possible if the diameter of the growing rod did not exceed 10 mm. Fig. 3b) shows the separated single crystalline part of the grown rod, which is homogeneous without any shiny (001) planes on the surface. This part has a size of 10 mm in diameter and 23 mm in length. Laue measurements at both cutting ends confirmed the segment of the rod to be a single crystal grown along the c -axis without any tilting. The crystal that was grown at a rate of 0.4 mm h^{-1} will be used as substrate material for the growth of PdCoO_2 films by molecular-beam epitaxy.

4. Discussion

Like other delafossites, CuFeO_2 is known to melt incongruently. This means the solid (with $\text{Cu:Fe} = 1:1$) is not in equilibrium with a liquid of the same composition. Typically the melting behavior is described to be peritectic, which means that upon heating in addition to melt with different composition some

higher melting solid phase is formed. For CuAlO_2 , $\alpha\text{-Al}_2\text{O}_3$ is the higher melting phase, and in some recent publications Fe_2O_3 is claimed to play this role for CuFeO_2 [25, 26]. This assumption is, however, incorrect because Fe_2O_3 decomposes to Fe_3O_4 and cannot be treated as a stable component of the system. Instead Cu, Fe and O_2 should be chosen as system components, see e.g. Fig. 1 in Ref. [23].

More detailed FactSage [24] calculations of the melting behavior of the Cu–Fe–O system are shown in Fig. 4. In the left phase diagram a fixed copper concentration of 52 mol-% is assumed, which is only a small Cu excess over Fe. On the right rim a “melt” phase field exists were the whole system forms a single copper-iron-oxide melt around $\log_{10}[p(\text{O}_2)/\text{bar}] \approx -2.5$. Upon cooling from this melt either Fe_2O_3 or Fe_3O_4 crystallizes first, depending on the oxygen fugacity. (For high p_{O_2} or high Cu excess the spinel $\text{Cu}^+\text{Fe}_2^{3+}\text{O}_4$ can also crystallize first.) The primary crystallization of iron oxide from Cu:Fe=1:1 mixtures was also observed experimentally (Fig. 1) and depletes the melt of iron.

A thermodynamic assessment of the complete Cu–Fe–O system is beyond the scope of this paper. Such assessments have been provided by Khvan et al. [32] and more recently by Shishin et al. [33]. Irrespective of differences in the models that are used by these authors, they agree on several key points that are relevant for the current crystal growth experiments. First, at temperatures between 1100–1400 K the delafossite CuFeO_2 is stable only for medium oxygen fugacities $\approx 10^{-7} - 10^{-1}$ bar, which overlaps well with the experimental conditions of this study. Second, the melt consists basically of Cu^+ , Cu^{2+} , Fe^{2+} , Fe^{3+} and O^{2-} . Minor amounts of Cu^0 and Fe^0 are present for metal-rich melts. Cu^{3+} , which was reported under very high oxygen pressure [34], can be neglected under the growth conditions we use in this study.

The authors of reference [33] include several of the authors of the FactSage [24] thermodynamic system, and consequently the FactSage calculations that are used in the present paper are in good agreement with both prior assessments [32, 33] — except the circumstance that FactSage so far contains no data for Cu^{2+} (CuO) in the melt. Nevertheless, under the growth conditions for CuFeO_2

the CuO content was found to be low, $< 10\%$ [2], which agrees well with the literature (see Fig. 16 in Ref. [33]). Consequently, these current FactSage calculations give a realistic description of the growth experiments.

The “CuFeO₂+melt” phase field has no connection to “melt” because the delafossite melts peritectically. Depletion of the melt by iron, however, shifts the Cu:Fe ratio towards larger values. In Fig. 4b) the Cu concentration is increased to 60 mol-% and this higher copper concentration leads to significantly lower liquidus temperatures. Between 1220 °C and 1192 °C both phase fields are directly connected and along this curve CuFeO₂ crystallizes first. In typical binary concentration vs. temperature ($x - T$) phase diagrams peritectics are horizontal (isotherm) lines in the diagram; this is not so here where $p(\text{O}_2)$ influences the temperature where the solid crystallizes.

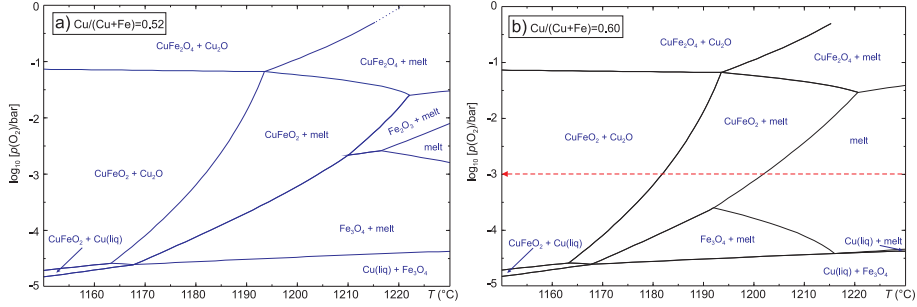


Figure 4: Predominance phase diagram of the system Cu–Fe–O₂ for a molar Cu concentration of a) 52%; b) 60%. The red (dashed) arrow at $\log_{10}[p(\text{O}_2)/\text{bar}] = -3$ is explained in Fig. 5.

Fig. 5 (which should be read from the right to the left) analyzes the crystallization path that is marked by a red dashed arrow in Fig. 4b). For the sake of simplicity, only the relative amounts (in moles) of Fe(II) oxide and Fe(III) oxide in the melt, the corresponding molar fraction of Fe₂O₃(melt), and the amounts (in moles) of solid CuFeO₂ and Cu₂O are shown. It is evident that above the 1202 °C liquidus the amount of Fe₂O₃(melt) rises slightly at the expense of FeO(melt) because a lower temperature shifts the equilibrium to higher valency. The first solid to crystallize is thus CuFeO₂, which contains only Fe³⁺. With cooling below 1202 °C, not only does the fraction of Fe₂O₃(melt) decrease, but

so does FeO(melt). Obviously additional free oxygen must be absorbed from the gas phase to oxidize FeO to Fe₂O₃, from which the delafossite finally forms. After passing the left boundary of the “CuFeO₂+melt” phase field at 1081 °C, the melt disappears completely and solid Cu₂O + additional CuFeO₂ crystallize together. This corresponds to the eutectic point in a standard $x - T$ phase diagram.

Note that the oxygen fugacity $\log_{10}[p(\text{O}_2)/\text{bar}] = -3$ used for the calculation of Fig. 5 is expected to be close to the true conditions used in the crystal growth experiments. In the ideal case, one can assume that 5N (99.999%) Ar contains oxygen background impurities around 2×10^{-6} bar, which sets a lower boundary on the oxygen partial pressure used during growth [35]. The leaks in the growth chamber and out-gassing of chemicals and constructed parts will further increase the oxygen level. But even if the estimated oxygen fugacity is incorrect by one or two orders of magnitude, or if the database and our own thermodynamic values [2, 24] that were used for the calculation of Figs. 4 and 5 would be somewhat erroneous, the general topology is not significantly changed. Hence, these figures are expected to give a realistic model.

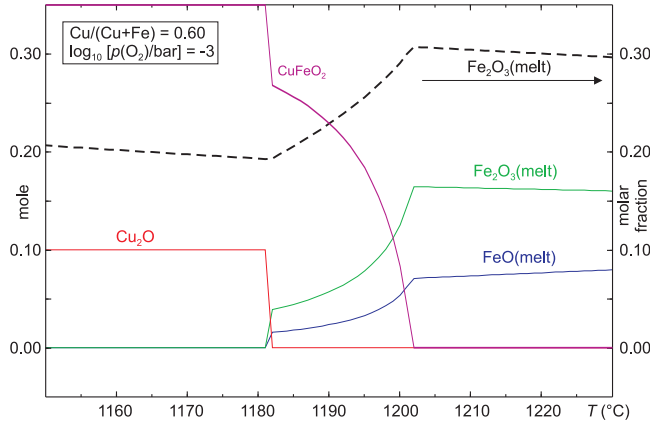


Figure 5: Crystallization of the Cu-Fe-oxide melt that is shown in Fig. 4b) under a constant oxygen fugacity of 1 mbar: Even if only CuFe³⁺O₂ starts to crystallize around 1200 °C, the amount of Fe²⁺O in the melt drops.

Copper can exist in the melt with oxidation states +2, +1 and 0, as shown

in Fig. 6 of [22], but with recent thermodynamic data for copper oxide melts [2] one finds that, under the conditions of CuFeO_2 growth, $> 90\%$ of the copper atoms are Cu^+ , which is the same valency as in the solid.

The importance of the gas phase to the crystal growth process is not restricted to the delafossite CuFeO_2 ; during the growth of the delafossite CuAlO_2 , the gas phase is also significantly involved. Fig. 4 in our recent paper [22] shows DTA/TG heating curves for several $\text{Cu}_2\text{O}-\text{Al}_2\text{O}_3$ mixtures, and the peritectic melting of CuAlO_2 can clearly be seen as an endothermic peak near $1230 - 1250^\circ\text{C}$ for the samples with 6% and 10% Al_2O_3 . The melting peak is always accompanied by a small mass gain. If $\text{Cu}^+\text{Al}^{3+}\text{O}_2$ melts, Al^{3+} maintains its oxidation state. Cu^+ is partially oxidized to Cu^{2+} because a deep eutectic (ca. 150 K below the congruent melting point of pure Cu_2O) appears between Cu_2O and CuO where the melt is entropically stabilized [34]. This means that upon cooling to achieve crystal growth, CuO must be partially reduced to Cu_2O , releasing free oxygen. Beyond the unfavorable position of the peritectic and eutectic points in this system, the permanent production of free oxygen at the phase boundary is detrimental to crystal growth. This is in contrast to the Cu-Fe-O system described here, because the necessary oxidation of Fe^{2+} to Fe^{3+} can be performed without the formation of gas. For the growth of CuFeO_2 the oxygen production that would result from $\text{Cu}^{2+} \rightarrow \text{Cu}^+$ reduction is likely compensated by the $\text{Fe}^{2+} \rightarrow \text{Fe}^{3+}$ oxidation. Indeed, during DTA/TG experiments, no mass change is observed during melting or crystallization, because the O_2 exchange with the atmosphere is insignificant. Another potential explanation for the lack of mass change could be the partial incorporation of Cu^{2+} into the delafossite structure, which was observed e.g., for $\text{LaCuO}_{2.5+x}$ and $\text{YCuO}_{2.5+x}$ delafossites [36]. A significantly different oxidation behavior of $\text{Cu}^+\text{B}^{3+}\text{O}_2$ delafossites for different B^{3+} ions was reported elsewhere [37].

5. Conclusions

Using the OFZ technique single crystals of CuFeO_2 with diameters up to 10 mm are grown. These are the largest synthetic delafossite single crystals ever grown and have sufficient size and quality for the preparation of wafers for the epitaxial deposition of thin films of other functional delafossites. The growth is performed from stoichiometric rods prepared from 1:1 (molar) mixtures of Cu_2O and Fe_2O_3 in an argon atmosphere. The melting behavior of CuFeO_2 is almost peritectic, by which we mean that the material CuFeO_2 crystallizes from a melt that is enriched in $\text{Cu}_2\text{O}/\text{CuO}$. A low but significant oxygen fugacity (≈ 1 mbar) must be available in the growth atmosphere to oxidize Fe^{2+} , which is partially present in the melt, to Fe^{3+} which is incorporated into the growing CuFeO_2 crystal. Hence, the melting behavior of CuFeO_2 is not simply peritectic (which would mean that two solid phases are in equilibrium with the melt). Rather the gas phase is also involved in the crystallization process, which makes crystal growth more complex and requires comparably low growth rates (cf. Table 1).

Acknowledgments

A. Kwasniewski is acknowledged for performing X-ray powder analysis and Laue measurements. We are indebted to C. Guguschev who performed energy-dispersive Laue mappings and X-ray fluorescence spectroscopy and to S. Ganschow for continuous support of this work. The authors acknowledge funding by the German Research Foundation (DFG) under project SI 463/9-1. D.G.S. acknowledges funding provided by the Alexander von Humboldt Foundation for his sabbatical stay at the Leibniz-Institut für Kristallzucht and support from the U.S. Department of Energy, Office of Basic Sciences, Division of Material Sciences and Engineering, under Award No. DE-SC0002334.

References

- [1] C. Friedel, Sur une combinaison naturelle des oxydes de fer et de cuivre, et sur la reproduction de l'atacamite, *Comptes Rendus (Paris)* 77 (1873) 211–214.
- [2] N. Wolff, Untersuchungen zur Züchtung von CuAlO_2 -Einkristallen, Ph.D. thesis, Technische Universität Berlin, Germany (2019).
- [3] J. Töpfer, M. Trari, P. Gravereau, J. P. Chaminade, J. P. Doumerc, Crystal growth and reinvestigation of the crystal structure of crednerite, CuMnO_2 , *Z. Krist.* 210 (1995) 184–187. doi:10.1524/zkri.1995.210.3.184.
- [4] R. D. Shannon, D. B. Rogers, C. T. Prewitt, Chemistry of noble metal oxides. I. Syntheses and properties of ABO_2 delafossite compounds, *Inorg. Chem.* 10 (1971) 713–718. doi:10.1021/ic50098a011.
- [5] C. W. Hicks, A. S. Gibbs, A. P. Mackenzie, H. Takatsu, Y. Maeno, E. A. Yelland, Quantum oscillations and high carrier mobility in the delafossite PdCoO_2 , *Phys. Rev. Lett.* 109 (2012) 116401. doi:10.1103/PhysRevLett.109.116401.
- [6] H. Takatsu, S. Yonezawa, S. Mouri, S. Nakatsuji, K. Tanaka, Y. Maeno, Roles of high-frequency optical phonons in the physical properties of the conductive delafossite PdCoO_2 , *J. Phys. Soc. Japan* 76 (2007) 104701. doi:10.1143/JPSJ.76.104701.
- [7] P. Kushwaha, V. Sunko, P. J. W. Moll, L. Bawden, J. M. Riley, N. Nandi, H. Rosner, M. P. Schmidt, F. Arnold, E. Hassinger, T. K. Kim, M. Hoesch, A. P. MacKenzie, P. D. C. King, Nearly free electrons in a 5d delafossite oxide metal, *Science Advances* 1 (2015) e1500692–e1500692.
- [8] R. Daou, R. Fresard, V. Eyert, S. Hebert, A. Maignan, Unconventional aspects of electronic transport in delafossite oxides, *Science and Technology of Advanced Materials* 18 (2017) 919–938.

- [9] V. Sunko, H. Rosner, P. Kushwaha, S. Khim, F. Mazzola, L. Bawden, O. J. Clark, J. M. Riley, D. Kasinathan, M. W. Haverkort, T. K. Kim, M. Hoesch, J. Fuji, I. Vobornik, A. P. MaxKenzie, P. D. C. King, Maximal rashba-like spin splitting via kinetic-energy-coupled inversion-symmetrie breaking, *Nature* 549 (2017) 492–496.
- [10] H. Kawazoe, H. Yanagi, K. Ueda, H. Honoso, Transparent p-type conducting oxides: Design and fabrication of p-n heterojunctions, *MRS Bull.* 25 (2000) 28–36.
- [11] H. Kawazoe, M. Yasukawa, H. Hyodo, M. Kurita, H. Yanagi, H. Hosono, P-type electrical conduction in transparent thin films of CuAlO_2 , *Nature* 389 (1997) 939–942. doi:10.1038/40087.
- [12] C. T. Prewitt, R. D. Shannon, D. B. Rogers, Chemistry of noble metal oxides. ii. crystal structures of PtCoO_2 , PdCoO_2 , CuFeO_2 , and AgFeO_2 , *Inorg. Chem.* 10 (1971) 719–723.
- [13] D. B. Rogers, R. D. Shannon, C. T. Prewitt, J. L. Gillson, Chemistry of noble metal oxides. iii. electrical transport properties and crystal chemistry of ABO_2 compounds with the delafossite structure, *Inorg. Chem.* 10 (1971) 723–727.
- [14] F. Capasso, Band-gap engineering: From physics and materials to new semiconductor devices, *Science* 235 (1987) 172–176. doi:10.1126/science.235.4785.172.
- [15] D. G. Schlom, L.-Q. Chen, C. J. Fennie, V. Gopalan, D. A. Muller, X. Q. Pan, R. Ramesh, Elastic strain engineering of ferroic oxides, *MRS. Bull.* 39 (2014) 118–130. doi:10.1557/mrs.2014.1.
- [16] R. Ramesh, D. G. Schlom, Creating emergent phenomena in oxide superlattices, *Nat. Rev. Mater.* 4 (2019) 257–268.
- [17] M. Brahlek, G. Rimal, J. M. Ok, D. Mukherjee, A. R. Mazza, Q. Lu, H. N. Lee, T. Z. Ward, R. R. Unocic, G. Eres, S. Oh, Growth of metallic

- delafossite PdCoO₂ by molecular beam epitaxy, *Phys. Rev. Mater.* 3 (2019) 093401. doi:10.1103/PhysRevMaterials.3.093401.
- [18] T. Harada, K. Fujiwara, A. Tsukazaki, Highly conductive PdCoO₂ ultrathin films for transparent electrodes, *APL Mater.* 6 (2018) 046107. doi:10.1063/1.5027579.
- [19] P. Yordanov, W. Sigle, P. Kaya, M. E. Grunder, R. Pentcheva, B. Keimer, H. U. Habermeier, Large thermopower anisotropy in PdCoO₂ thin films, *Phys. Rev. Mater.* 3 (2019) 085403. doi:10.1103/PhysRevMaterials.3.085403.
- [20] J. Lewis, D. Schwarzenbach, H. D. Flack, Electric field gradients and charge density in corundum, α -Al₂O₃, *Acta Cryst. A* 38 (1982) 733–739. doi:10.1107/S0567739482001478.
- [21] A. P. Mackenzie, The properties of ultrapure delafossite metals, *Rep. Prog. Phys.* 80 (2017) 032501. doi:10.1088/1361-6633/aa50e5.
- [22] N. Wolff, D. Klimm, D. Siche, Thermodynamic investigations on the growth of CuAlO₂ delafossite crystals, *J. Solid State Chem.* 258 (2018) 495–500. doi:10.1016/j.jssc.2017.11.014.
- [23] N. Wolff, D. Klimm, S. Ganschow, D. Siche, Thermodynamic investigation of ternary delafossite crystals, *Cryst. Res. Technol.* 54 (2019) 1900036. doi:10.1002/crat.201900036.
- [24] www.factsage.com, FactSage 7.4, GTT Technologies, Kaiserstr. 100, 52134 Herzogenrath, Germany (2019).
- [25] T. Zhao, M. Hasegawa, M. Koike, H. Takei, Crystal growth of CuFeO₂ by the floating-zone method, *J. Cryst. Growth* 148 (1995) 189–192. doi:https://doi.org/10.1016/0022-0248(94)00881-7.
- [26] J. Song, J. Wu, X. Rao, S. Li, Z. Zhao, X. Liu, X. Zhao, X. Sun, Single crystal growth of CuFe_{1-x}Ga_xO₂ by the opti-

- cal floating-zone method, *J. Cryst. Growth* 446 (2016) 79–84. doi:<https://doi.org/10.1016/j.jcrysgro.2016.04.046>.
- [27] T. Zhao, M. Hasegawa, H. Takei, Growth and characterization of CuFeO_2 single crystals, *J. Cryst. Growth* 154 (1995) 322–328. doi:[https://doi.org/10.1016/0022-0248\(95\)00172-7](https://doi.org/10.1016/0022-0248(95)00172-7).
- [28] T. Zhao, M. Hasegawa, H. Takei, Crystal growth and characterization of cuprous ferrite (CuFeO_2), *J. Cryst. Growth* 166 (1996) 408–413. doi:[https://doi.org/10.1016/0022-0248\(95\)00520-X](https://doi.org/10.1016/0022-0248(95)00520-X).
- [29] S. Kato, S. Suzuki, M. Ogasawara, Synthesis and reversible oxidation/reduction behavior of delafossite-type $\text{CuCr}_{1-x}\text{Al}_x\text{O}_2$, *J. Mater. Sci.* 52 (2017) 10718–10725. doi:[10.1007/s10853-017-1263-7](https://doi.org/10.1007/s10853-017-1263-7).
- [30] A. Mohan, B. Büchner, S. Wurmehl, C. Hess, Growth of single crystalline delafossite LaCuO_2 by the travelling-solvent floating zone method, *J. Cryst. Growth* 402 (2014) 304–307. doi:[10.1016/j.jcrysgro.2014.06.023](https://doi.org/10.1016/j.jcrysgro.2014.06.023).
- [31] C. Guguschev, R. Tagle, U. Juda, A. Kwasniewski, Microstructural investigations of SrTiO_3 single crystals and polysilicon using a powerful new X-ray diffraction surface mapping technique, *J. Appl. Cryst.* 48 (2015) 1883–1888. doi:[10.1107/0021899515000000](https://doi.org/10.1107/0021899515000000).
- [32] A. V. Khvan, O. B. Fabrichnaya, G. Savinykh, R. Adam, H. J. Seifert, Thermodynamic assessment of the Cu–Fe–O system, *J. Phase Equilib. Diff.* 32 (6) (2011) 498–511. doi:[10.1007/s11669-011-9951-5](https://doi.org/10.1007/s11669-011-9951-5).
- [33] D. Shishin, T. Hidayat, E. Jak, S. A. Decterov, Critical assessment and thermodynamic modeling of the Cu–Fe–O system, *Calphad* 41 (2013) 160–179. doi:[10.1016/j.calphad.2013.04.001](https://doi.org/10.1016/j.calphad.2013.04.001).
- [34] L. Schramm, G. Behr, W. Löser, K. Wetzig, Thermodynamic reassessment of the Cu–O phase diagram, *J. Phase Equilib. Diff.* 26 (2005) 605–612. doi:[10.1361/154770305X74421](https://doi.org/10.1361/154770305X74421).

- [35] D. Klimm, S. Ganschow, The control of iron oxidation state during FeO and olivine crystal growth, *J. Cryst. Growth* 275 (2005) e849–e854. doi:10.1016/j.jcrysgro.2004.11.080.
- [36] R. Cava, H. Zandbergen, A. Ramirez, H. Takagi, C. Chen, J. Krajewski, W. Peck, J. Waszczak, G. Meigs, R. Roth, L. Schneemeyer, $\text{LaCuO}_{2.5+x}$ and $\text{YCuO}_{2.5+x}$ delafossites: Materials with triangular $\text{Cu}_{2+\delta}$ planes, *J. Solid State Chem.* 104 (1993) 437–452. doi:10.1006/jssc.1993.1179.
- [37] A. P. Amrute, Z. Lodziana, C. Mondelli, F. Krumeich, J. Pérez-Ramírez, Solid-state chemistry of cuprous delafossites: Synthesis and stability aspects, *Chem. Mater.* 25 (21) (2013) 4423–4435. doi:10.1021/cm402902m.